

Using the Reactions $\text{O} + \text{H}_2 \rightarrow \text{OH} + \text{H}$ to Explore the Importance of the Atomic Quantum States on Chemical Kinetics and Reaction Dynamics

João Brandão, Wenli Wang, Carolina M. A. Rio*

CIQA, Department of Chemistry and Pharmacy, Faculty of Science and Technology, University of the Algarve, Campus of Gambelas, Portugal

Copyright © 2015 Horizon Research Publishing All rights reserved.

Abstract The $\text{O} + \text{H}_2$ reaction is a particular example to alert the importance of a clear definition of the quantum state of an atom when referring to a chemical reaction. In its ground state, $\text{O} (^3\text{P})$, the oxygen atom reacts with H_2 through an energy barrier with small rate constant. In contrast, when the oxygen atom is in its first excited state, $\text{O} (^1\text{D})$, the reaction $\text{O} + \text{H}_2$ occurs without energy barrier and the rate constant is seven orders of magnitude higher. The dynamic behaviour of this reaction depends also on the quantum state of the oxygen atom.

Keywords Quantum State, Rate Constant

1. The Quantum State of the Oxygen Atom and Reactions $\text{O} + \text{H}_2$

Textbooks of General Chemistry and introductory Physical Chemistry usually pay attention to the electronic configuration of an atom, but few care for the description of their quantum states and their spectroscopic levels arising from spin-orbit coupling, considering these topics as a curiosity with few chemical interest. Nevertheless, when teaching chemical kinetics, and in particular the atmospheric chemistry reactions, we face a table of elementary reactions where the kinetic data depends on the quantum states of reactants.

The oxygen atom is a good example to illustrate this behaviour. The study of the oxygen atom is similar to the one of the carbon atom illustrated in most textbooks. At the ground electronic configuration $1s^2 2s^2 2p^4$, there are fifteen different microstates corresponding to the ^3P , ^1D and ^1S quantum states (or terms), which are identified as belonging to the $^3\text{P}_{2,1,0}$, $^1\text{D}_2$ and $^1\text{S}_0$ levels, as illustrates in Figure 1. Using Hund's rules, the ground energy level is identified as the $^3\text{P}_2$. Due to spin-orbit interaction, the two other levels of this state, the $^3\text{P}_1$ and $^3\text{P}_0$, are only 158.265 cm^{-1} and 226.977

cm^{-1} higher, respectively. But the $^1\text{D}_2$ level is $15867.862 \text{ cm}^{-1}$ while the $^1\text{S}_0$ level is $33792.583 \text{ cm}^{-1}$ above the ground level.

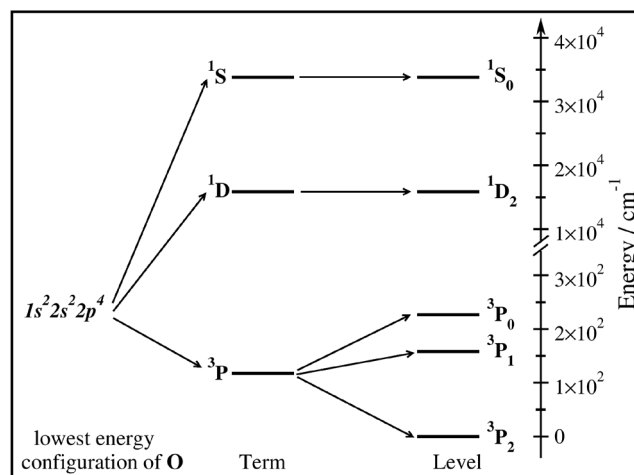


Figure 1. Energy Levels of Neutral Oxygen at ground electronic configuration.

Atomic oxygen is one of the most chemically reactive species in the atmosphere and all the three states oxygen are present throughout most of the atmosphere as results of photochemical and ionic processes. For example, when stratospheric ozone is irradiated with solar radiation, the quantum state of the oxygen atom product strongly depends on the wavelength of the incident radiation. The product will be mainly $\text{O} (^1\text{D})$ if the wavelength is less than 310 nm (ultraviolet radiation) and $\text{O} (^3\text{P})$ otherwise. The $\text{O} (^1\text{D})$ atom can react with any other species present in the stratosphere and, by this way, alter the concentration of odd oxygen in the Chapman cycle of ozone¹⁻⁴. Among those reactions, the reaction of $\text{O} (^1\text{D})$ with molecular hydrogen is one of those whose incertitude most contributes to errors in the modulation of atmospheric chemistry. In addition to its role in atmospheric chemistry, the reaction of $\text{O} (^3\text{P})$ with molecular hydrogen is one of the main reactions in combustion chemistry. As a result, the reactions $\text{O} (^1\text{D}, ^3\text{P}) +$

$\text{H}_2 \rightarrow \text{OH} + \text{H}$ have been subject of several experimental and theoretical studies⁵⁻¹⁹.

Experimental results clearly show that kinetic of the reaction between oxygen atom and molecular hydrogen depends on the quantum states of reactants. When search the kinetic data for these reactions, two kind of very different rate constants can be found. At temperature 298K, the recommended rate constant for $\text{O}(^1D) + \text{H}_2$ is $1.1 \times 10^{-10} \text{ cm}^3 \text{ molecule}^{-1} \text{ s}^{-1}$ (Ref. 20). At the same temperature rate constant for $\text{O}(^3P) + \text{H}_2$ is $9.0 \times 10^{-18} \text{ cm}^3 \text{ molecule}^{-1} \text{ s}^{-1}$ (Ref. 21). For reaction $\text{O}(^3P) + \text{H}_2$, the rate constant increases with temperature and can be fit into Arrhenius equation with positive activation energy. While for the reaction $\text{O}(^1D) + \text{H}_2$, the rate constant is not sensible to temperature and even negative activation energy was found²².

2. The Detailed Interaction between O Atom and H_2 Molecule

Theoretically, the differences in kinetic behaviour between the reactions $\text{O}(^3P) + \text{H}_2$ and $\text{O}(^1D) + \text{H}_2$ can be well understood through the detailed interaction between O atom and H_2 molecule. Within the framework of Born-Oppenheimer approximation, these two reactions occur on different potential energy surfaces (PES). The Figure 2 shows the correlation diagram for the interaction of an O atom with ground state H_2 .

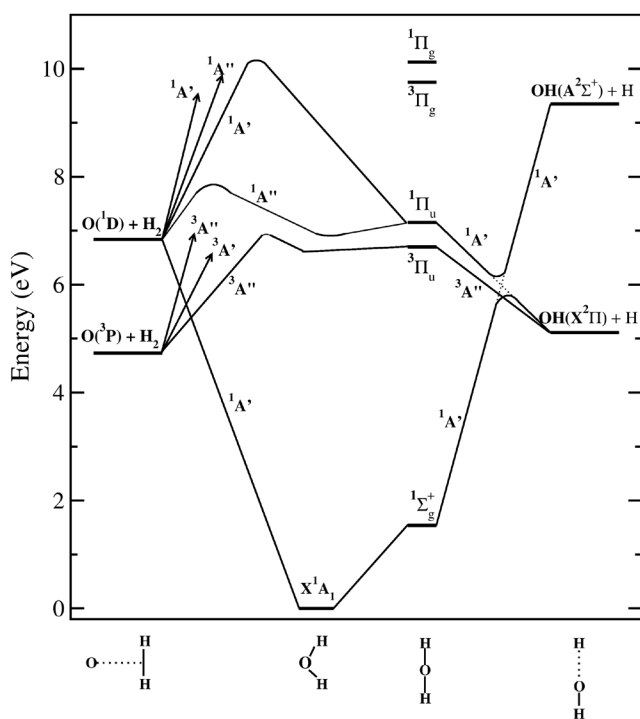


Figure 2. Correlation diagram of the potential energy surfaces involved in the $\text{O} + \text{H}_2$ reaction, adapted from Ref. 14.

When the $\text{O}(^3P)$ atom approaches ground state $\text{H}_2(^1\Sigma_g^+)$, they give rise to three triplet PESs, two of symmetry A'' and one A' in the C_s point group. Here, the prime means that the

wave function keeps its sign when reflected on the plane of the three atoms while the double prime means a change of sign in the same operation. These can, somehow, be viewed as if the double occupied p orbital stays in that plane being each one of the single occupied orbitals in the perpendicular position (changing sign by reflection), otherwise the double occupied orbital can be perpendicular to that plane and the wave function doesn't change sign by reflection.

In collinear configurations, where it is located the saddle point for the title reaction, this reflection is no longer a symmetry operation and one A'' (the one with a single occupied p orbital pointing to the H_2 molecule) and the $^3A'$ surfaces became degenerate in a $^3\Pi$ surface, labelled according to the $C_{\infty v}$ point group. The other $^3A''$, with the double occupied orbital pointing to the H_2 , will correlate with a $^3\Sigma$ PES. This last Σ surface correspond to a most favourable orientation of the quadrupole moment of the O atom and is lower in energy at larger O $\cdots \text{H}_2$ collinear distances (in the van der Waals region) but, due to the double occupancy of that orbital, it doesn't favour the formation of the OH diatomic and has a higher energy barrier to reaction. In addition, this Σ PES correlates with the product OH diatomic in its first excited state, $\text{OH}(^2\Sigma)$ and does not contribute to the title reaction at the energies of chemical practical interest. The two degenerate Π PESs have the same energy barrier and give OH products in their ground electronic state, $\text{OH}(^2\Pi)$, and should be considered when studying this reaction.

When the $\text{O}(^1D)$ atom approaches ground state $\text{H}_2(^1\Sigma_g^+)$, five singlet potential energy surfaces are accessible for reactants. The mainly contribution comes from the lowest ($^1A'$) PES, that correlates without energy barrier with the (1A_1) ground state of the H_2O molecule. The other four PESs present an energy barrier to reaction. However the first excited state, $1A''$, must be considered for energies higher than 3.5 kcal/mol or temperatures above 1000 K.

At collinear geometries, the ground surface is labelled $^1\Sigma^+$. It has been noted that, due to the non-adiabatic electrostatic coupling between this state and the $^1\Pi$, where the $^1A'$ and $^1A''$ states of lower energy are degenerate, the cross section receives a contribution from the $^1\Pi$ state of approximately 10%. The other two singlet potential energy surfaces correlate with a $^1\Delta$ state at collinear geometries and present a higher energy barrier. So, they do not contribute to reaction at the energies of chemical interest.

To illustrate the main differences between these reactions, here we use two of our published PESs^{23,24} for singlet and triplet state of this system as examples. The Figure 3 is a three dimensional view of an $\text{O}(^3P)$ atom around an equilibrium H_2 . There we can see a barrier in all approaching angles and that the shallow van der Waals valley favours a collinear attack in this PES. The approaching of an $\text{O}(^1D)$ atom to an equilibrium H_2 is shown in Figure 4. Note the lack of energy barrier at perpendicular angles. The very small energy barrier of 0.1 kcal/mol at collinear geometries is hardly viewed at the scale of this figure. The deep well corresponds to the H_2O equilibrium molecule if we allow the

H—H distance to extend. The minimum reaction pathway for both reactions is compared in Figure 5. It is clear that the ground state Oxygen atom reacts with H_2 through a barrier while the reaction $\text{O}(^1D) + \text{H}_2$ is barrierless.

It is also important to teach students that the reaction of a ground state O atom with H_2 doesn't produce H_2O , but OH plus H. This is clearly stated when teaching the mechanism of H_2 combustion, where the H_2O is formed on the reaction of OH with H_2 , but it is not clear for a student of General Chemistry.

We must state that the ground state O atom is a triplet state and, in a reaction with a singlet state molecule, it can't produce a singlet state product by spin conservation rules, or, in a language more accessible to students, a ground state oxygen atom has two electrons with the same spin and the hydrogen molecule has two electrons with opposite spins, being impossible to build a molecule with two new bonds having two electrons of opposite spin each.

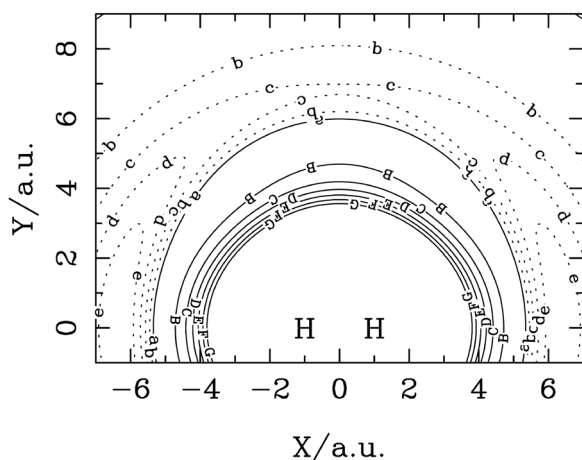


Figure 3. Contour plot for an $\text{O}(^3P)$ atom around an equilibrium H_2 molecule. The solid lines start at 0 kcal/mol, are equally spaced by 1 kcal/mol. Starting at 0 kcal/mol and equally spaced by -0.1 kcal/mol, the dashed lines depict the van der Waals regions.

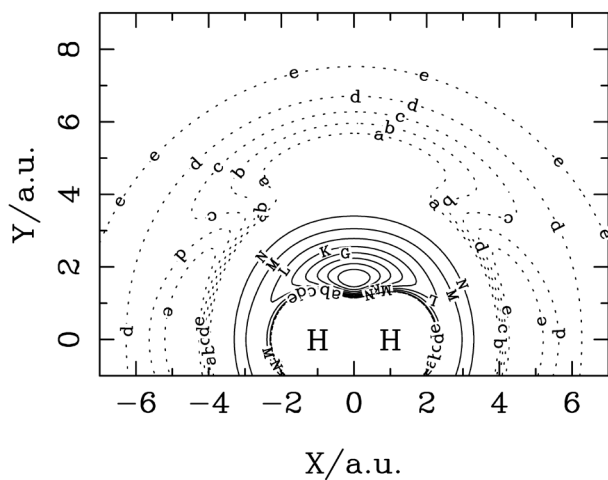


Figure 4. Contour plot for an $\text{O}(^1D)$ atom around an equilibrium H_2 molecule. The solid contours are equally spaced by 0.02 Eh, starting at -0.3704 Eh, dashed contours are equally spaced by 0.1 kcal/mol, the contour labelled by f corresponds to the dissociation energy.

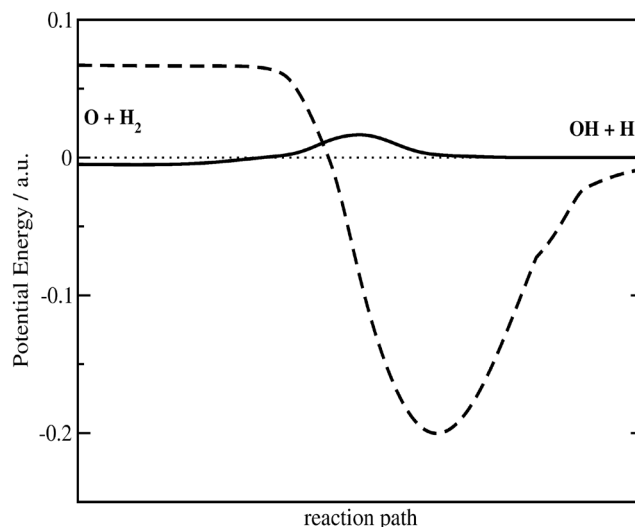


Figure 5. Reaction path for the title reactions. The solid line represents the $\text{O}(^3P) + \text{H}_2 \rightarrow \text{OH} + \text{H}$ and the dashed line $\text{O}(^1D) + \text{H}_2 \rightarrow \text{OH} + \text{H}$

Only an oxygen atom in his first singlet state can produce a water molecule in reaction with hydrogen. However this highly excited water molecule will dissociate into products, or reactants, before being deactivated by collision or emission of radiation.

3. A Reaction Dynamics

Besides as good example for elucidating the importance of the quantum state of chemical elements in chemical kinetics, the title reactions provide good examples for teaching dynamics of elementary bimolecular reactions. We have studied theoretically these reactions in the past^{13,19,23-25}, and here, using some of our previous trajectories calculations results, we can show that two different types of dynamical behaviour can be exemplified by these two reactions.

For a bimolecular reaction of a three-particle system, a simple and instructive way to find the dynamical behaviour is to plot the interatomic distances as a function of time. Typically, for a direct reaction the switch over between the old bond and new bonds occurs within a very short time interval, corresponding to about one vibrational period. Figure 6 is such a plot for a reactive trajectory of reaction $\text{O}(^3P) + \text{H}_2$. Clearly this is a reactive collision of the 'direct' type.

On the other hand an indirect reaction occurs via a long-lived complex. Figure 7 display a representative reactive collision of an Oxygen atom in the 1D state. In this case, the mechanism of reaction involves an insertion of oxygen atom into the middle of the H_2 bond and formation of an excited H_2O molecule that experiments several rotations and vibrations prior to dissociation into products. Indeed, the reaction $\text{O}(^1D) + \text{H}_2$ is usually considered as a prototype of an indirect type insertion reaction.

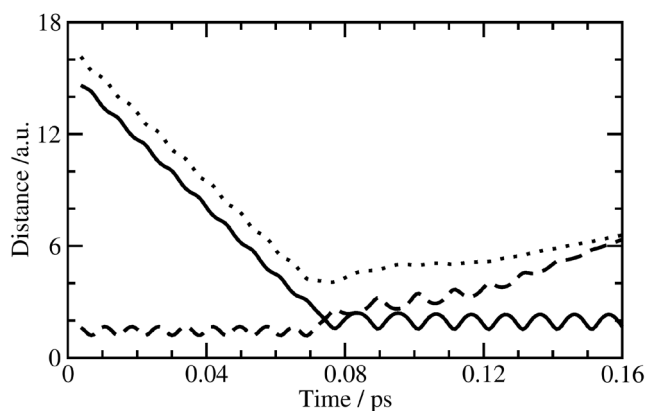


Figure 6. Distance vs. time plot for a reactive trajectory of the reaction $O(^3P) + H_2 \rightarrow OH + H$ at the collision energy 13.7 kcal/mol. The line — represents one OH diatomic, - - - refers to the HH diatomic and the other OH diatomic.

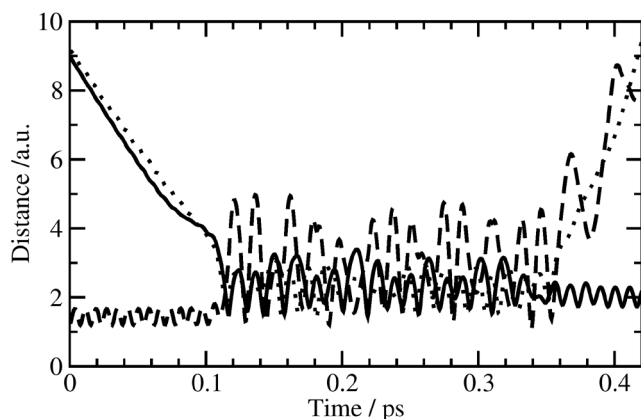


Figure 7. Distance vs. time plot for a reactive trajectory of the reaction $O(^1D) + H_2 \rightarrow OH + H$ at the collision energy 3.0 kcal/mol. The line — represents one OH diatomic, - - - refers to the HH diatomic and the other OH diatomic.

For an indirect reaction, as a result of the long-lived complex formation, the product quantum states distribution will not depend directly on the reactant states and collision energy. It is expected that the long-lived complexes should statistically redistribute the total energy. Table 1 shows some results of our statistical calculations of the energy distribution of the reaction $O(^1D) + H_2$ using phase space theory²⁶. For the same collision energies, our QCT results are indicated in Table 2, and agree reasonably well with our statistical calculations.

Table 1. Distribution, in percentage, of the total energy in translational, vibrational and rotational energies of the products of the reaction $O(^1D) + H_2$, using phase space calculations²⁵.

$E_{col}/\text{kcal mol}^{-1}$	$E_{tr}(\%)$	$E_{vib}(\%)$	$E_{rot}(\%)$
0.5	36.83	41.12	22.06
1.0	36.74	39.97	23.28
1.3	36.71	39.60	23.69
1.9	36.76	38.67	24.53
3.0	37.30	37.56	25.14
5.0	38.42	36.10	25.48

Table 2. Distribution, in percentage, of the total energy in translational, vibrational and rotational energies of the products of the reaction $O(^1D) + H_2$, using QCT results²⁵.

$E_{col}/\text{kcal mol}^{-1}$	$E_{tr}(\%)$	$E_{vib}(\%)$	$E_{rot}(\%)$
0.5	30.15	34.56	35.29
1.0	29.40	34.42	36.16
1.3	29.44	35.06	35.5
1.9	29.75	34.26	35.99
3.0	30.12	35.13	34.75
5.0	31.24	35.62	33.14

As results of the direct and indirect nature of these reactions, direct reaction and indirect reactions have different pattern for angular distribution of the reaction products. A direct reaction should produce forward or backward products, while an indirect one with a long-lived complex will dissociates with equal probability in all directions, presenting a forward-backward symmetric distribution. Figure 8 displays representative differential cross sections for the reaction $O(^3P) + H_2$. Here the reaction shows a forward angular distribution of reaction products which is in accordance with the direct reaction mechanism. For reaction $O(^1D) + H_2$, the angular distribution of the reaction products is represented in Figure 9, and is a forward-backward symmetric distribution. This corresponds to the expected behaviour for an indirect reaction.

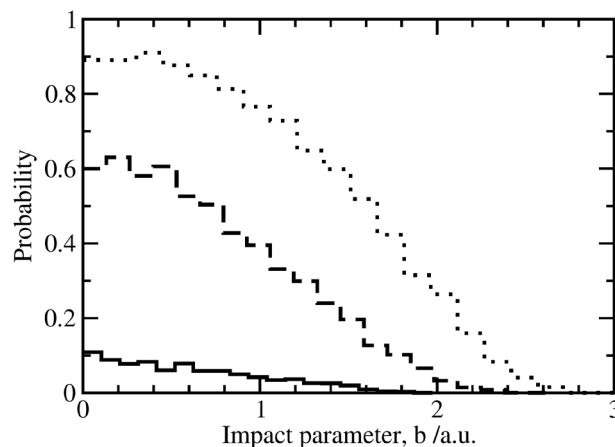


Figure 8. Differential cross sections for the reaction $O(^3P) + H_2 \rightarrow OH + H$, at the collision energy 20.0 kcal/mol.

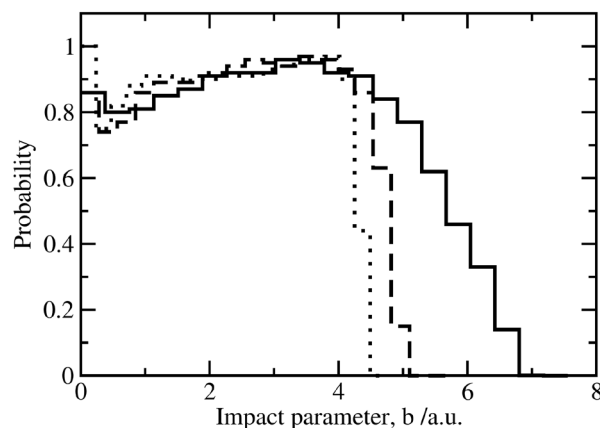


Figure 9. Differential cross sections for the reaction $O(^1D) + H_2 \rightarrow OH + H$, at the collision energy 3.0 kcal/mol.

Another interesting view of the difference between the reactions $\text{O}(^3P) + \text{H}_2$ and $\text{O}(^1D) + \text{H}_2$ is the opacity function that describes the reaction probability, $P(b)$, as a function of the impact parameter. Figure 10 displays opacity functions for reaction $\text{O}(^3P) + \text{H}_2$ at three different collision energies. Since this is a reaction with a potential energy barrier, the $P(b)$ increases with collision energy. Because of the centrifugal barrier, the reaction probability decrease while increasing the impact parameters. In the case of the $\text{O}(^1D) + \text{H}_2$ reaction the picture is quite different as shown in Figure 11. For all impact parameters, the reaction probability remains close to unity up to a b_{max} value for which the probability dramatically decreases, with the exception of the highest collision energy (3.0 kcal/mol) where the reaction probability decreases more smoothly with b . Also the maximum impact parameter has a very different value for both reactions. The $\text{O}(^1D)$ reaction has a large impact parameter characteristic of reactions without barrier dominated by long-range forces. In contrast the $\text{O}(^3P)$ reaction has a much shorter maximum impact parameter, which denotes a reaction dominated by an energy barrier.

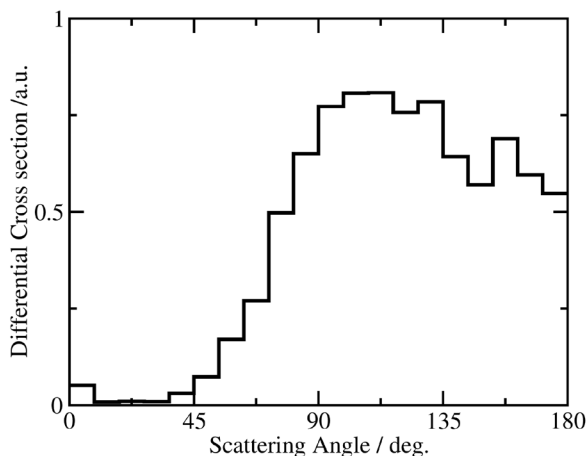


Figure 10. Opacity functions for the reaction $\text{O}(^3P) + \text{H}_2 \rightarrow \text{OH} + \text{H}$. Lines —, - - - and ••• correspond to the 13.7, 20.0 and 30.0 kcal/mol collision energies, respectively.

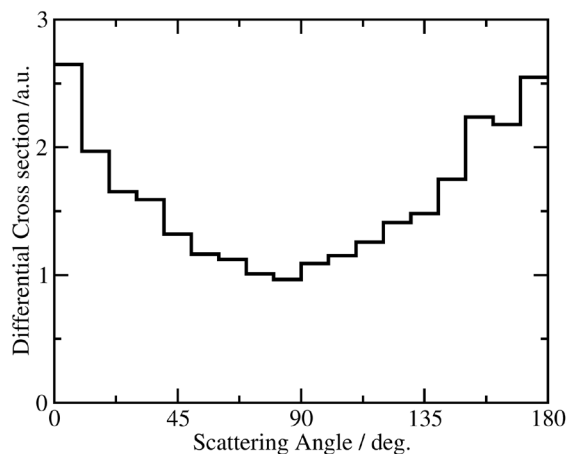


Figure 11. Opacity functions for the reaction $\text{O}(^1D) + \text{H}_2 \rightarrow \text{OH} + \text{H}$. Lines —, - - - and ••• correspond to the 0.5, 1.3 and 3.0 kcal/mol collision energies, respectively.

4. Conclusions

The $\text{O} + \text{H}_2$ reaction, of overwhelming importance in combustion and atmospheric chemistry, is often mentioned in the textbook on chemical kinetics and physical chemistry. The rate constant of this reaction depends strongly on the oxygen atom quantum state. The comparison between the reactions with oxygen atom on 3P and 1D quantum states allows students to understand the importance of a clear definition of the quantum state of an atom in chemical reaction. Students gain insight into the interaction between O atom and H_2 molecule.

In addition, these reactions provide good examples for teaching bimolecular reaction dynamics: The ground state oxygen atom, $\text{O}(^3P)$, reacts with H_2 through a barrier and following a direct mechanism. But in the excited state, $\text{O}(^1D)$, the reaction is barrierless and proceed via the formation of a long-lived reaction complex.

REFERENCES

- [1] Chamberlain, J. W.; Hunten, D. M. *Theory of Planetary Atmospheres - An Introduction to Their Physics and Chemistry*; Academic Press, Inc., 1987.
- [2] Barker, J. R. In *Progress and Problems in Atmospheric Chemistry*, World Scientific ed., 1995; pp 1-33.
- [3] BaSeinfeld, J. H. In *Progress and Problems in Atmospheric Chemistry*, World Scientific ed., 1995; pp 34-57.
- [4] Sander, S. P.; Friedl, R. R.; Ravishankara, A. R.; Golden, D. M.; Kolb, C. E.; Kurylo, M. J.; Molina, M. J.; Moortgat, G. K.; Keller-Rudek, H.; Finlayson-Pitts, B. J.; Wine, P. H.; Huie, R. E.; Orkin, V. L. *Chemical Kinetics and Photochemical Data for Use in Atmospheric Studies*; JPL Publication 06-2, NASA-Jet Propulsion Laboratory, Pasadena, California, 2006.
- [5] Alagia, M.; Balucani, N.; Cartechini, L.; Casavecchia, P.; van Kleef, E. H.; Volpi, G. G.; Kuntz, P. J.; Sloan, J. J. Crossed molecular beams and quasiclassical trajectory studies of the reaction $\text{O}(^1D) + \text{H}_2(\text{D}_2)$. *J. Chem. Phys.* 1998, 108, 6698-6708.
- [6] Hsu, Y.-T.; Liu, K.; Pederson, L. A.; Schatz, G. C. Reaction dynamics of $\text{O}(^1D) + \text{HD}$. I. The insertion pathway. *J. Chem. Phys.* 1999, 111, 7921-7930.
- [7] Ahmed, M.; Peterka, D. S.; Suits, A. G. Crossed-beam reaction of $\text{O}(^1D) + \text{D}_2 \rightarrow \text{OD} + \text{D}$ by velocity map imaging. *Chem. Phys. Lett.* 1999, 301, 372-378.
- [8] Buss, R. J.; Casavecchia, P.; Sibener, S. J.; Lee, Y. T. Reactive Scattering of $\text{O}(^1D) + \text{H}_2$. *Chem. Phys. Lett.* 1981, 82, 386-391.
- [9] Drukker, K.; Schatz, G. C. Quantum scattering study of electronic Coriolis and nonadiabatic coupling effects in $\text{O}(^1D) + \text{H}_2 \rightarrow \text{OH} + \text{H}$. *J. Chem. Phys.* 1999, 111, 2451-2463.
- [10] Varandas, A. J. C.; Voronin, A. I.; Caridade, P. J. S. B.; Riganelli, A. Is there a barrier for C_{2v} insertion reaction in

- $O(^1D)+H_2$? A test dynamics study based on two-valued energy-switching potential surfaces. Chem. Phys. Lett. 2000, 331, 331-338.
- [11] Aoiz, F. J.; Banares, L.; Castillo, J. F.; Herrero, V. J.; Martinez-Haya, B.; Honvault, P.; Launay, J. M.; Liu, X.; Lin, J. J.; Harich, S. A.; Wang, C. C.; Yang, X. The $O(^1D) + H_2$ reaction at 56 meV collision energy: A comparison between quantum mechanical, quasiclassical trajectory, and crossed beam results. J. Chem. Phys. 2002, 116, 10692-10703.
- [12] Takayanagi, T. Nonadiabatic quantum reactive scattering calculations for the $O(^1D) + H_2$, D_2 , and HD reactions on the lowest three potential energy surfaces. J. Chem. Phys. 2002, 116, 2439-2446.
- [13] Brandão, J.; Rio, C. M. A. Long-range interactions within the H_2O molecule. Chem. Phys. Lett. 2003, 372, 866-872.
- [14] Durand, G.; Chapuisat, X. An ab initio description of the excited states of the reaction $O(^3P, ^1D) + H_2 \rightarrow OH(^2\Pi, ^2\Sigma^+) + H$. Chem. Phys. 1985, 96, 381-407.
- [15] Gardon, D. J.; Minton, T. K.; Maiti, B.; Troya, D.; Schatz, G. C. A crossed molecular beams study of the $O(^3P)+H_2$ reaction: Comparison of excitation function with accurate quantum reactive scattering calculations. J. Chem. Phys. 2003, 118, 1585-1588.
- [16] Maiti, B.; Schatz, G. C. Theoretical studies of intersystem crossing effects in the $O(^3P, ^1D) + H_2$ reaction. J. Chem. Phys. 2003, 119, 12360-12371.
- [17] Braunstein, M.; Adler-Golden, S.; Maiti, B.; Schatz, G. C. Quantum and classical studies of the $O(^3P)+H_2(v=0-3, j=0) \rightarrow OH+H$ reaction using benchmark potential surfaces. J. Chem. Phys. 2004, 120, 4316-4323.
- [18] Balakrishnan, N. Quantum calculations of the $O(^3P) + H_2 \rightarrow OH + H$ reaction. J. Chem. Phys. 2004, 121, 6346-6352.
- [19] Wang, W.; Rosa, C.; Brandão, J. Theoretical studies on the $O(^3P) + H_2 \rightarrow OH + H$ reaction. Chem. Phys. Lett. 2006, 418, 250-254.
- [20] DeMore, W. B.; Sander, S. P.; Golden, D. M.; Hampson, R. F.; Kurylo, M. J.; Howard, C. J.; Ravishankara, A. R.; Kolb, C. E.; Molina, M. J. Chemical kinetics and Photochemical Data for Use in Stratospheric Modeling; JPL publication 97-4, NASA-Jet Propulsion Laboratory, 1997.
- [21] Atkinson, R.; Baulch, D. L.; Cox, R. A.; Hampson, Jr., R. F.; Troe, J. A. Evaluated kinetic and photochemical data for atmospheric chemistry. Supplement III. J. Phys. Chem. Ref. Data 1989, 18, 881.
- [22] Blitz, M. A.; Dillon, T. J.; Heard, D. E.; Pilling, M. J.; Trought, I. D. Phys. Chem. Chem. Phys. 2004, 6, 2162.
- [23] Brandão, J.; Mogo, C.; Silva, B. C. Potential energy surface for $H_2O(^3A'')$ from accurate ab initio data with inclusion of long-range interactions. J. Chem. Phys. 2004, 121, 8861-8868.
- [24] Brandão, J.; Rio, C. M. A. Double-valued potential energy surface for H_2O derived from accurate ab initio data and including long-range interactions. J. Chem. Phys. 2003, 119, 3148-3159.
- [25] Rio, C.; Brandão, J. Dynamical studies and product analysis of $O(^1D) + H_2/D_2$ reactions. Mol. Phys. 2007, 105, 359-373.
- [26] Pechukas, P.; Light, J. C.; Rankin, C. Statistical Theory of Chemical Kinetics: Application to Neutral-Atom-Molecule Reactions. J. Chem. Phys. 1966, 44, 794-805.